PROJECTIONS OF CLIMATE FORCING BY SULFATE, ORGANIC AEROSOLS, DUST, AND SEA SALT: RESULTS FROM THE IPCC MODEL INTER-COMPARISON WORKSHOP

Joyce E. Penner[1] and Yang Zhang[1]
[1]University of Michigan, Ann Arbor, Michigan

1.   INTRODUCTION

Comparisons of models with observations for sulfate aerosols and other sulfur compounds are particularly relevant for assessing model capabilities because the emissions of sulfur bearing compounds are better known than the emissions of other aerosol compounds. Thus, comparison can focus on the capabilities of the models to treat transport and oxidation processes. Recent field studies, however, have pointed out the importance of organic aerosol compounds [Hegg et al., 1997]; dust aerosols [Li and Prospero, 1998]; and sea salt aerosols [Murphy et al., 1998]. Moreover, the presence of absorbing aerosols, primarily in the form of soot, is important because it lowers the single scattering albedo of the aerosol, leading to a decrease in the reflection and an increase in the absorption of solar radiation. Furthermore, the magnitude of the indirect effect is sensitive to the abundance of natural aerosols represented in the models [Penner et al., 1999]. Therefore, an examination of model capability to represent this entire suite of aerosol components was undertaken as part of this report.

Emissions for this model comparison were specified by the most currently available emissions inventories for each component (see Table1). Ten aerosol models participated in the model inter-comparison of sulfate, eight treated black carbon, 7 treated organic carbon, 6 treated dust, and 5 treated sea salt. Eight scenarios were defined. The first, SC1, was selected to provide good estimates of present-day aerosol emissions. SC2 used present day chemistry and natural emissions to simulate aerosol concentrations in 2030 according to the IPCC SRES A2 scenario (SRES, 1999). SC3 used present day chemistry and natural emissions to simulate the A2 scenario in 2100 and SC4 used present day chemistry and natural emissions to simulate the B1 scenario in 2100. In addition, we examined possible future changes in emissions of the natural components DMS, terpenes, dust and sea salt in 2100 in SC5 for the A2 scenario and in SC7 for the B1 scenario. Scenario SC6, also examined changes in emissions of other gas phase components associated with the production of sulfate in the A2 scenario in 2100 (see Chapter 4). Finally, SC8 is provided to show estimates for anthropogenic emissions in 2100 associated with the IS92a scenario. Some of the participants also provided estimates of direct and indirect forcing. The estimates, together with the range of predicted concentrations among the models, help to define the uncertainty in aerosol forcing for future scenarios. Not all participants were capable of producing results for all 5 aerosol compounds. The models participants, scenarios they provided, and the aerosol components treated in each model are summarized in Table 2.

2. COMPARISON OF MODELED AND OBSERVED AEROSOL CONCENTRATIONS

Like previous model intercomparisons, the IPCC comparison showed vast differences in model prediction of the vertical distribution of aerosols. This is highlighted by comparison of the zonal average

Table 1. Prescribed annual source strength for emissions of gas phase aerosol precursors and primary emissions (Tg N or S or C per yr or Tg/yr).

Aerosol Precursors:	NH	SH	Global
SO2 (as Tg S/yr)			
Fossil fuel and industry	68	8	76
Aircraft (1992)	0.04	0.003	0.04
Biomass burning	1.2	1.0	2.2
Volcanoes	6.3	3.0	9.3
DMS or H2S (as Tg S/yr)			
Oceans	11	13	24
Land biota and soils	0.6	0.4	1.0
Volatile organic emissions (as Tg C/yr)			
Anthropogenic			109
Terpenes	67	60	127

Primary Emissions:	NH	SH	Global
Organic Matter (0-2 μm)			
Biomass burning	28.3	26.0	54.3
Fossil fuel	28.4	0.4	28.8
Black Carbon (0-2 μm)			
Biomass burning	2.9	2.7	5.6
Fossil fuel	6.5	0.1	6.6
Aircraft	0.005	0.0004	0.006
Industrial Dust, etc.			100
Biogenic (0-2 μm)			50
Sea Salt			
d< 1 μm	23	31	54
d=1-16 μm	1420	1870	3290
Total sea salt	1440	1900	3340
Mineral (Soil) Dust			
<1 μm	90	17	110
1-2 μm	240	50	290
2-20 μm	1470	282	1750
Total dust	1800	349	2150

Table 2 Aerosol models participating in IPCC model intercomparison workshop.

Code	Model	Contributor	Aerosol components treated	Scenarios	Forcing provided
1	Ulaq	Pitari	sulfate, OC, BC, dust, sea salt	SC1, SC2, SC3, SC4, SC5, SC7	
2	GISS	Koch	sulfate, OC, BC, dust, sea salt	SC1, SC2, SC3, SC4, SC8	direct, indirect
3	GSFC	Chin	sulfate, OC, BC, dust, sea salt	SC1, SC2, SC3, SC4	
4	Hadley Center	Roberts	sulfate, BC, dust	SC1, SC2, SC3, SC4, SC5	direct
5	LLNL/ U. Mich.	Chuang	sulfate, OC, BC, dust, sea salt	SC1, SC2, SC3, SC4, SC5, SC7	indirect
6	Max Planck/ Dalhousie U.	Feichter	sulfate, OC, BC	SC1, SC2, SC3	indirect
7	U. Michigan	Herzog	sulfate, OC, BC, dust, sea salt	SC1, SC2, SC3, SC4, SC5, SC7	direct
8	UKMO	Collins	sulfate	SC1,SC3	
9	NCAR/Mozart	Tie	sulfate, BC	SC1	
10	KNMI/TM3	van Weele	sulfate	SC1	

concentrations of aerosol sulfate in July from the different models. These differences are mainly the result of differences in vertical transport of both SO_2 and aerosol sulfate coupled with differences in the scavenging by precipitation associated with this transport. Despite these differences, however, the models did a reasonable job of simulating aerosol sulfate at most of the remote surface sites in our comparison. For example, Figure 1 shows a comparison between model predicted and observed annual average non-sea salt sulfate concentrations in the North and South Atlantic. The North Atlantic is a region dominated by anthropogenic sulfate and has source strengths for both anthropogenic and natural components that are reasonably well characterized. Except for the ECHAM model at high latitudes, all models are within a factor of 2 of observations in this region though they tend to be high and show more scatter in winter in remote regions. The ECHAM model was the only model to include the feedbacks between increases in anthropogenic sulfate concentrations and cloud microphysics and, in general, predicted much higher sulfate concentrations in polar regions compared to other models when run in this coupled manner The predicted sulfate concentration is similar to other models if the sulfate and cloud microphysics are treated as uncoupled. Thus, the comparison in Figure 1 may indicate that the appropriate representation of either the model cloud microphysics or the coupling of this microphysics with the sulfur cycle needs further development. We note, however, that the
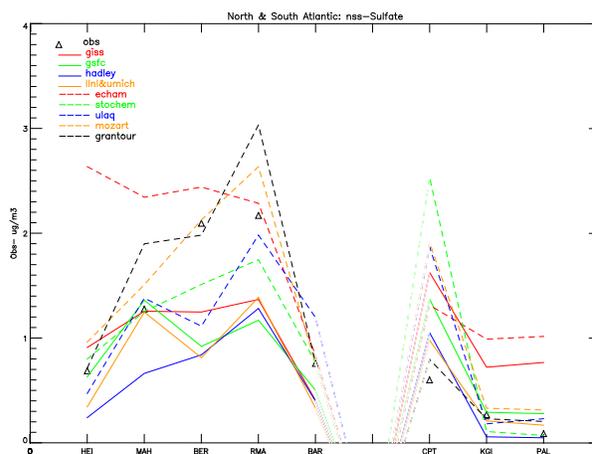
Figure 1. Observed and model-predicted annual average concentrations of non-sea salt sulfate (in $\mu g\ m^{-3}$) at a series of North and South Atlantic locations. The models are listed in Table 2. Data were those provided by Savoie and Prospero [private communication, 1999]. Stations refer to: Heimaey, Iceland (HEI); Mace Head, Ireland (MAH); Bermuda (BER); Miami, Florida (RMA); Ragged Point, Barbados (BAR); Cape Point, South Africa (CPT); King George Island (KGI);, and Palmer Station, Antarctica (PAL). All comparison with surface data are preliminary since some participants reported values at the surface, while others reported values that were the average of the mixing ratio from 0 to 2 km.

coupled model compares well with observations at other high latitude locations.

The reasonable simulations of surface sulfate concentrations by all models indicates that much of the differences in forcing reported in the literature is most likely associated with either variations in emissions, variations in the vertical distrubution of sulfate, or varying treatments of relative humidity within different models and the response of sulfate aerosols to variations in relative humidity (f(RH)) [Penner et al., 1999].
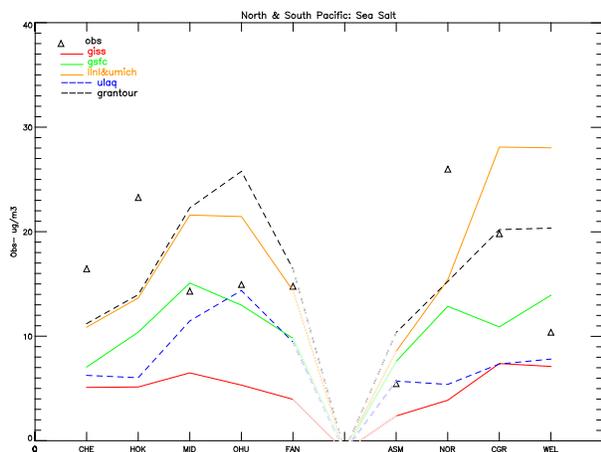
Figure.2. Observed and model-predicted annual average concentrations of sea salt (as Na) (in μg m^{-3}) at a series of stations in the North and South Pacific. The models are listed in Table 2. Data were those provided by Savoie and Prospero [private communication, 1999]. Stations refer to: Cheju, Korea (CHE); Hedo, Okinawa, Japan (HOK); Midway Island (MID); Oahu, Hawaii (OHU); Fanning Island (FAN); American Samoa (ASM); Norfolk Island (NOR); Cape Grim, Tasmania (CGR); and Wellington/Baring Head, New Zealand (WEL). All comparison with surface data are preliminary since some participants reported values at the surface, while others reported values that were the average of the mixing ratio from 0 to 2 km.

In contrast to sulfate, the IPCC comparison for other aerosol types showed that the capability for models to treat these components is relatively inferior to their capability to simulate sulfate aerosol. For example, for sea salt in the North and South Pacific, Figure 2 shows that the predicted sea salt from the LLNL/Umich and the ECHAM/Grantour model are high compared to observations at Midway, Oahu, and in New Zealand (MID, OHU, and WEL) but represent the sea salt concentrations reasonably well at Fanning Island (FAN) and Cape Grim (CGR). On the other hand the GISS model is low compared to observations at Midway, Oahu, and Cape Grim, but does a very good job at reproducing the observed concentrations in New Zealand. The GSFC model and ULAQ are intermediate.

Results were similar in the North and South Atlantic, except for King George Island and Palmer Station where all models predicted concentrations that were significantly higher than the observations. Either the source strength is too high at these high latitudes or the models' prediction of meridional transport is too strong or removal here is too weak.

For sea salt, Chin and Ginoux chose to implement the methodology of Gong et al. [1997] to produce consistent sea salt fluxes within the GSFC model—rather than to use the monthly average sea salt fluxes as determined by Gong et al. from the Canadian Climate Model. Higher sea surface wind speeds in the underlying meteorology model (Goddard Data Assimilation Office (DAO) model; e.g. the GEOS-1 DAS) produced annual average sea salt fluxes that were 55% higher than those from the Canadian model. Thus, overall sea salt fluxes are uncertain by at least this factor.

For dust in the Northern Hemisphere, the model-observation comparison showed that the GSFC and GISS models were consistently higher than the observations, while the Hadley model was in general too low. (The GISS and GSFC models, however, reported mixing ratios for 0 to 2 km, and this may bias the comparison with data at the surface). Ulaq and ECHAM/Grantour were each within a factor of 2 of the observations. In the Southern Hemisphere, except for the Hadley model, all models predict concentrations higher than the observations at all stations further south than Yate, New Caledonia (YAT, 22 S). Thus, it appears that dust mobilization estimates may be too high, particularly those for Australia and South America (Ginoux, private communication, 1999). The paucity of dust from these regions relative to other arid dust source areas has been noted previously [Prospero et al., 1989, Tegen and Fung 1994, Rea, 1994], and may reflect the relative tectonic stability, low weathering rates, duration of land surface exposure, and low human impacts in this area. Penner et al. [1999], for example, found better dust characterization with their model when the Australian source strength was decreased by a factor of 10.

The interpretation of the comparison of observed and model-predicted concentrations for both organic carbon and black carbon is relatively more difficult because of both inaccuracies in the observations due to poorly quantified analytical techniques (Section 5.2) and the fact that measured concentrations are only available on a campaign basis. In addition, the source strength of these compounds is more poorly known. Despite these difficulties, most models were able to reproduce the observed concentrations of BC to within a factor of 10 (see Figure 3) and some models (e.g. GISS, GSFC) were consistently better than a factor of 10. The comparison of measured and predicted OC is less satisfactory, but in this case measurements may not be

very representative and the emissions inventory may be particularly inaccurate.

In addition to the model comparison with observations, an analysis of the variation in aerosol burden among the models indicated that model results differed by factor of 3.3 for sulfate (10 models) and by a factor of 2 for organic carbon (5 models). In contrast, the range of total burdens for black carbon, dust, and sea salt was a factor of 17, 8, and 6, respectively. As a result, since the model-observation comparison for
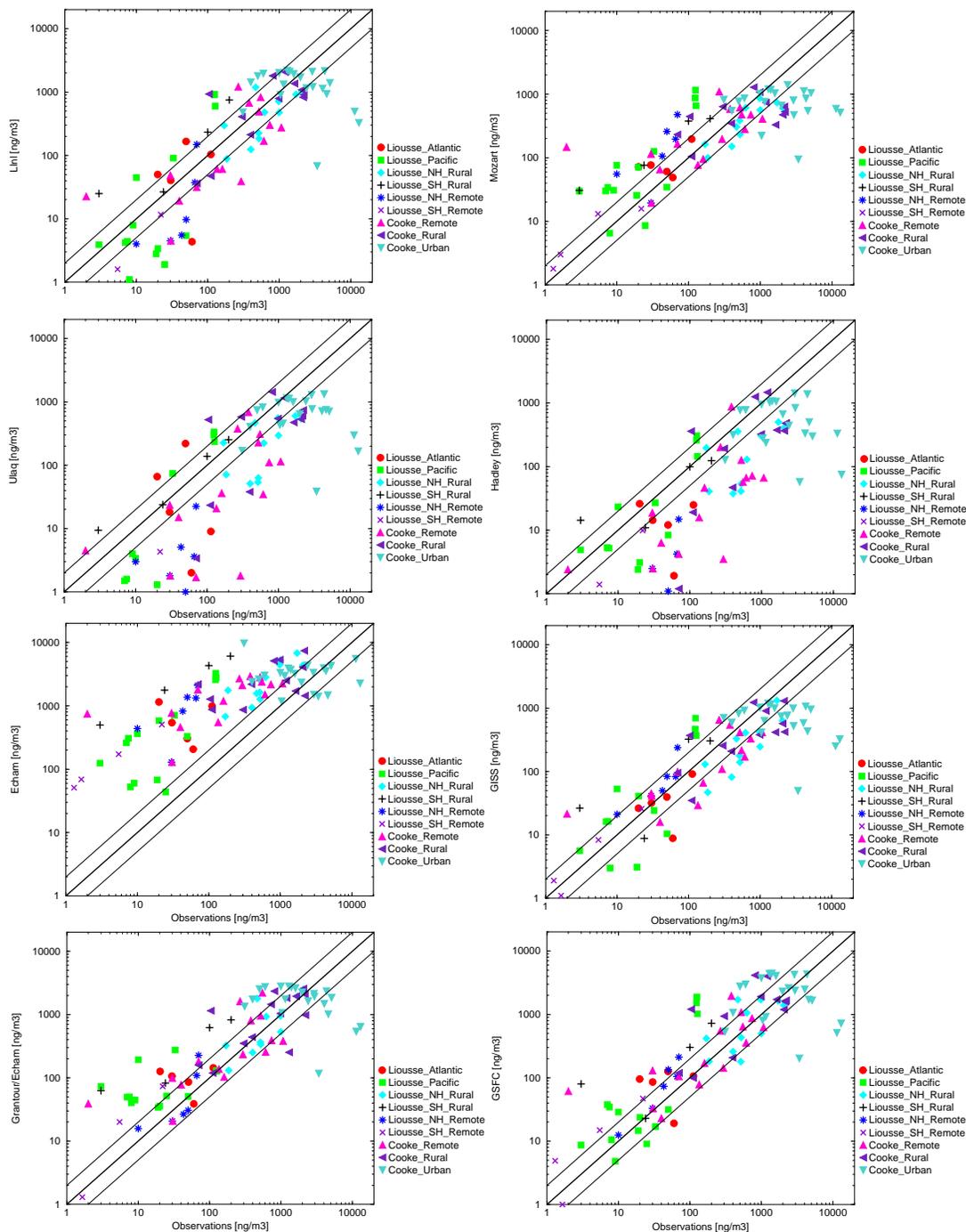
Figure 3. Observed and model-predicted concentrations of black carbon (in μgC m^{-3}) at a number of locations. Results are shown for the LLNL/Umich model (a); Mozart (b); Ulaq (c); the Hadley model (d); the Max Planck/Dalhousie model (e); the GISS model (f); the ECHAM/Grantour model (g); and the GSFC model (h). Observations refer to those summarized by Liousse et al. [1996]) and Cooke et al. [1999].

4

sulfate, dust, and sea salt is within a factor of 2 at most sites, we may conclude that, except for dust in the Southern Hemisphere, the total uncertainty associated with both emissions and the model capability to represent burden is about a factor of 2. For organic and black carbon, the model-observation comparison shows more variability, and the total uncertainty is about a factor of 10.

3. SIMULATION OF FUTURE AEROSOL CONCENTRATIONS AND FORCING

Of the models which participated in the IPCC Workshop, three calculated direct forcing and three calculated indirect forcing. For direct forcing, the Grantour/ECHAM model, the GISS model, and the Hadley Center models were used. The Grantour model was a version updated to use ECHAM 3.6 meteorological fields at 4-hour time resolution and T21 spatial resolution together with the parameterization for aerosol radiative forcing for sulfate, organic carbon, black carbon, and biomass aerosols described by Grant et al. [1999] (see also Penner et al. [1999]). The GISS model is that described by Koch et al [1999]. The Hadley Center model is that described by Jones et al. [1999]. For indirect forcing, the LLNL/Umich model [Chuang et al., 1999; Penner et al. 1999a], the GISS model, and the ECHAM/Dalhousie [Lohmann et al., 1999a] models were used. The LLNL/Umich model uses the mechanistic formulation for the determination of droplet concentration described by Chuang et al. [1997] but has been updated to include interactive dust and sea salt as described in Penner et al. [1999]. This model does not include prognostic treatment for water and therefore provides a strict estimate of forcing by the Twomey mechanism alone (i.e. the first indirect effect). The GISS model used an empirical formulation for relating droplet concentrations and aerosol concentrations. The ECHAM/Dalhousie model used the mechanistic formulation of Chuang et al. [1997] as described in Lohmann et al. [1999a,b] and included consideration of the second indirect effect. In addition, the ECHAM/Dalhousie model used monthly averaged dust and sea salt fields from the LLNL/Umich model as described in Penner et al. [1999].

The models used in the forcing calculations used different formulations for the treatment of precipitation scavenging of organic and black carbon aerosols. The Grantour/ECHAM model used a mechanistic formulation of scavenging in large-scale and convective precipitation, with the mixing ratio of aerosol mass incorporated into liquid water (or released upon evaporation) proportional to the mixing ratio of water condensed. No aging for the properties of black and organic carbon was assumed. The GISS model assumed that black carbon would only become hygroscopic only after deposition of H2SO4 formed from the oxidation of SO2. The LLNL/Umich model

assumed the formulation described in Penner et al. (1998), with no aging properties for any of the aerosols. The ECHAM/Dalhousie model assumed that initially 50% of organic carbon and 80% of black carbon was hydrophobic but would become hydrophylic after an e-folding time of 40 hours [Lohmann et al., 1999a]. The Hadley model assumed an aging for BC in which it becomes hydrophilic with an e-folding time of 1.6 days.

Partly as a result of these assumptions, concentrations and predicted forcings differed significantly. For example, despite the fact that Lohmann et al. [1999c] and Chuang et al. [1999] used identical emissions inventories and formulations for the effect of hygroscopic organic carbon on initial droplet concentrations, their predictions for the first indirect effect (the Twomey effect) differ significantly. Thus, Chuang et al. [1999] find a total forcing by carbonaceous aerosols of -1.44 Wm^{-2} whereas Lohmann et al. [1999c] find a forcing for the combined first and second effects of only -0.9 Wm^{-2} associated with carbonaceous aerosols. Similarly, whereas, the GISS model calculation for black carbon yields a total burden that is only 20% higher than that in the LLNL/Umich model in the simulations for the year 2000, for the year 2100, the predicted concentration in the GISS model is 90% higher than that in the LLNL/Umich model under the A2 scenario.

In addition to the estimates for forcing provided by workshop participants, two additional studies were performed. In these studies, the A2 2100 emission scenario was used to simulate HNO$_3$ concentrations in 2100 using the University of Olso model (see Chapter 4) and the present day NH$_3$ emissions were scaled by the increase in N$_2$O emissions 2100 from the SRES A2 scenario. Then the models described by Adams et al. [1999] and Penner et al. [1999a,c] were used to estimate direct forcing after condensation of the additional HNO$_3$ and NH$_3$ onto the calculated sulfate aerosol. The estimated forcing increased to -3.03 Wm^{-2} in the Adams et al. model. This model is based on the GISS model but gets somewhat larger forcing for SO$_4^{2-}$ even with the same sulfate burden because of difference assumptions about the amount of water uptake. Even so, most of the projected increase in forcing in 2100 is caused by a significant increase in NH$_3$ emissions (factor of 2.4 increase over 2000) and the projected increase in HNO$_3$ associated with increased NO$_x$ emissions (factor of 3.4 increase over 2000).

4. DISCUSSION

The estimates for current-day (2000) direct sulfate forcing as well as those for future scenarios differ by about a factor of 3 between the models, consistent with the variation in estimates from models in the literature (see Chapter 6), and consistent with the computed differences in sulfate abundance. By 2100, BC

emissions, however, could dominate the total direct forcing, resulting in a net positive direct forcing by anthropogenic aerosols, particularly if the forcing by BC were treated as an internal mixture. As an internal mixture, BC absorbs almost twice as much radiation as it does when treated externally. Thus, it increase could easily lead to an additional positive forcing of order 1 Wm^{-2}. Projected increases in nitrate and ammonium,

Table 3. Direct forcing estimated by different models for the IPCC SRES scenarios (Wm^{-2}).

		GISS	Hadley	Grantour/ ECHAM	Adams et al. (1999)	Penner et al. (1999c)
2000	SO4=	-0.66	-0.18		-1.29	
	BC	0.51	0.13			
	OC	-0.29				
	Total	-0.44				
A2 2030	SO4=	-1.25	-0.31			
	BC	0.63	0.17			
	OC	-0.40				
	Total	-1.02				
A2 2100	SO4=	-0.54	-0.18		-2.32	
	BC	2.02	0.30			
	OC	-0.69				
	Total	0.79				
B1 2100	SO4=	-0.32	-0.10			
	BC	0.73				
	OC					
	Total					
IS92a 2100	SO4=					
	BC					
	OC					
	Total					

Table 4. Indirect forcing (short wave) estimated by different models for the IPCC SRES scenarios.

	LLNL/Umich	GISS	ECHAM/ Dalhousie
2000	-0.73	-1.56	-0.30
A2 2030	-0.97	-1.85	
A2 2100	-1.20	-1.92	-0.11
B1 2100	-0.63		
2100 "Natural aerosols"	-1.16[1]		
IS92a 2100			

[1]This is an estimate from the difference in cloud forcing between two simulations. New calculations are underway to provide more accurate estimates.

however, could easily offset this warming. Thus the net change in the projected direct forcing by aerosols is likely to lie between 0 and –1 Wm^{-2} in 2100. Up to 2030, however, according to the A2 scenario, direct forcing by aerosols may continue to mask somewhat the projected warming from greenhouse gases.

The estimates for the current-day (2000) indirect forcing by the LLNL/Umich model and that by the ECHAM/Dalhousie model are smaller than similar estimates made prior to the workshop [Penner et al., 1999a; Lohmann et al. 1999c]. The decrease in the LLNL/Umich estimates of forcing (from –1.44 Wm^{-2} to –0.73 Wm^{-2}) are consistent with the larger sub-micron dust and sea salt emissions specified here. The

decrease in the ECHAM/Dalhousie model estimates of forcing is associated with the fact that the aerosols were treated as fully interactive with the cloud microphysics in these simulations. The change is caused by a different vertical profile of Δ CDNC and Δ LWC (Liquid Water Content) (Lohmann, private communication, 1999) in these simulations.

The indirect forcing is projected to increase in both the LLNL/Umich model and the GISS model through 2100 according to the A2 scenario, associated primarily

with the assumed continued increases in emissions of carbon aerosols. The decrease calculated for the ECHAM/Dalhousie model in 2100 may be the result of changing oxidant concentrations. Calculations of sulfate aerosol abundance that included the effects of changing oxidant concentrations by the ULAQ model project small decreases in both sulfate and carbon aerosols if the effects of oxidant changes are included.

Most natural aerosols are projected here to increase only slightly on a global and annual average basis. DMS increases cause an increase in sulfate burden of only 1% in the A2 scenario in 2100 according to the LLNL/Umich model. Sub-micron dust concentrations increase 3%, and organic aerosols from increased terpene emissions cause an increase in organic aerosol burden of 3%. Thus, the projected changes in anthropogenic emissions continue to dominate the changes in aerosol abundance for these species. The largest projected increase in "natural" aerosols is that due to increases in sea salt. Sea salt concentrations increase by 74% in 2100 in the LLNL/Umich model.

At the time of this writing, we did not have an adequate measure of the effect of this increase. But estimates for direct forcing imply a possible additional forcing of up to -0.8 Wm^{-2} due to sea salt aerosols. The indirect forcing associated with these increased emissions may be estimated from twice the difference between the anthropogenic aerosols forcing for the SC5 and SC3 scenarios and for the SC7 and SC4 scenarios. This yields a total forcing of between -0.3 and -0.5 Wm^{-2} associated with future increases in sea salt emissions. New calculations are underway to better characterize this forcing.

5. REFERENCES

Adams, P.J., J.H. Seinfeld and D.M. Koch, 1999: Global concentrations of tropospheric sulfate, nitrate, and ammonium aerosol simulated in a general circulation model. *J. Geophys. Res.,* 104, 13,791-13,823.

Chuang, C.C., J.E. Penner, K.E. Taylor, A.S. Grossman, and J.J. Walton, 1997: An assessment of the radiative effects of anthropogenic sulfate, *J. Geophys. Res.*, 102, 3761-3778.

Chuang, C. C., J. E. Penner, and G. E. Grant, 1999: The effect of anthropogenic aerosols on cloud susceptibility: A sensitivity study to aerosol characteristics and global concentrations. To be submitted to *J. Geophys. Res.*

Gong, S.L., L.A. Barrie, and J.-P. Blanchet, 19997: Modeling sea-salt aerosols in the atmosphere. Part 1: Model development, J. Geophys. Res. 102, 3805-3818.

Grant, K.E., C.C. Chuang, A.S. Grossman, and J.E. Penner, Modeling the spectral optical properties of ammonium sulfate and biomass burning aerosols; Parameterization of relative humidity effects and model results, 1999: *Atmos. Env.*, 33, 2603-2620.

Hegg, D. A., J. Livingston, P. V. Hobbs, T. Novakov, and P. Russell, 1997: Chemical apportionment of aerosol column optical depth off the mid-Atlantic coast of the United States, *J. Geophys. Res.*, 102, 25,293-25,303.

Jones, A., D. L. Roberts and M. J. Woodage, 1999, The indirect effects of anthropogenic sulphate aerosol simulated using a climate model with an interactive sulfur cycle. *Q. J. Roy. Met. Soc.,* In review.

Koch et al., 1999: J. Geophys. Res., 104, 23,799-23,823.

Li-Jones, X., and J. M. Prospero, 1998: Variations in the size distribution of non-sea-salt sulfate aerosol in the marine boundary layer at Barbados: Impact of African dust, *J. Geophys. Res.*, 103, 16073-16084.

Liousse, C., J. E. Penner, C. Chuang, J. J. Walton, H. Eddleman, and H. Cachier, 1996: A global three-dimensional model study of carbonaceous aerosols, *J. Geophys. Res.*, *101*, 19,411-19,432.

Lohmann, U., J. Feichter, C.C. Chuang, and J.E. Penner, 1999a: Prediction of the number of cloud droplets in the ECHAM GCM, *J. Geophys. Res.*, 104, 9169-9198.

Lohmann, U., J. Feichter, C.C. Chuang, and J.E. Penner, 1999b: Erratum, *J. Geophys. Res.*, in press.

Lohmann, U., J. Feichter, J.E. Penner, and R. Leaitch, 1999c: Indirect effect of sulfate and carbonaceous aerosols: A mechanistic treatment, submitted to J. Geophys. Res.

Murphy, D. M., J. R. Anderson, P. K. Quinn, L. M. McInnes, F. J. Brechtel, S. M. Kreidenweis, A. M. Middlebrook, M. Posfai, D. S. Thompson, and P. R. Buseck, 1998: Influence of sea-salt on aerosol radiative properties in the Southern Ocean marine boundary layer, *Nature*, 392, 62-65.

Penner, J.E., Chuang, C.C., and K. Grant, 1999a: Climate Change and Radiative Forcing by Anthropogenic Aerosols: Research Findings During the Last 5 Years, La Jolla International School of Science, submitted, The Institute for Advanced Physics Studies, La Jolla, CA 92038-2946, March 29-30, 1999a.

Penner, J.E., Y. Feng, W.W. Pan, and M. Jacobson, 1999b: Climate forcing by anthropogenic aerosols: Impacts from nitrate and ammonium, in preparation.

Prospero, J.M., M. Uematsu, and D.L. Savoie, 1989: Mineral aerosol transport to the Pacific Ocean, in *Chemical Oceanography*, J.P. Riley, and R. Chester, Eds., Academic, London, 188-218.

Rea, D.K. *,* 1994: The paleoclimatic record provided by eolian deposition in the deep sea: The geologic history of wind, *Rev. Geophys.*, *i32,* 159-195.

Tegen, I., and I. Fung, , 1994: Modeling of mineral dust in the atmosphere: Sources, transport, and optical thickness, *J. Geophys. Res., 99*, 22,897-22,914.